

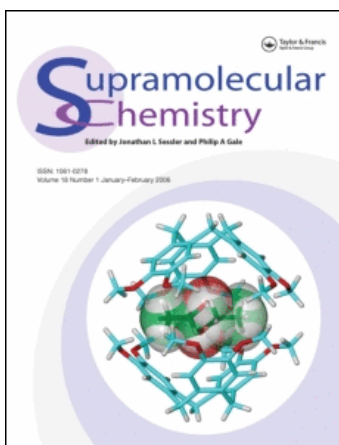
This article was downloaded by:

On: 29 January 2011

Access details: *Access Details: Free Access*

Publisher *Taylor & Francis*

Informa Ltd Registered in England and Wales Registered Number: 1072954 Registered office: Mortimer House, 37-41 Mortimer Street, London W1T 3JH, UK



## Supramolecular Chemistry

Publication details, including instructions for authors and subscription information:

<http://www.informaworld.com/smpp/title~content=t713649759>

### Molecular recognition by cyclodextrins: the x-ray structure of 6<sup>A</sup>-boc-L-phenylalanyl-amino-6<sup>A</sup>-deoxy-β-cyclodextrin

M. Selkti<sup>a</sup>; H. Parrot Lopez<sup>b</sup>; J. Navaza<sup>a</sup>; F. Villain<sup>a</sup>; C. de Rango<sup>a</sup>

<sup>a</sup> UPR 180 CNRS, Centre Pharmaceutique, Université Paris-Sud, Chtenay-Malabry, France <sup>b</sup> URA 1843 CNRS, Centre Pharmaceutique, Université Paris-Sud, Chtenay-Malabry, France

**To cite this Article** Selkti, M. , Lopez, H. Parrot , Navaza, J. , Villain, F. and de Rango, C.(1995) 'Molecular recognition by cyclodextrins: the x-ray structure of 6<sup>A</sup>-boc-L-phenylalanyl-amino-6<sup>A</sup>-deoxy-β-cyclodextrin', *Supramolecular Chemistry*, 5: 4, 255 – 266

**To link to this Article:** DOI: 10.1080/10610279508233952

**URL:** <http://dx.doi.org/10.1080/10610279508233952>

PLEASE SCROLL DOWN FOR ARTICLE

Full terms and conditions of use: <http://www.informaworld.com/terms-and-conditions-of-access.pdf>

This article may be used for research, teaching and private study purposes. Any substantial or systematic reproduction, re-distribution, re-selling, loan or sub-licensing, systematic supply or distribution in any form to anyone is expressly forbidden.

The publisher does not give any warranty express or implied or make any representation that the contents will be complete or accurate or up to date. The accuracy of any instructions, formulae and drug doses should be independently verified with primary sources. The publisher shall not be liable for any loss, actions, claims, proceedings, demand or costs or damages whatsoever or howsoever caused arising directly or indirectly in connection with or arising out of the use of this material.

# Molecular recognition by cyclodextrins: the x-ray structure of 6<sup>A</sup>-*boc*-L- phenylalanyl-amino-6<sup>A</sup>-deoxy- $\beta$ - cyclodextrin

M. SELKTI\*<sup>1</sup>, H. PARROT LOPEZ<sup>2</sup>, J. NAVAZA<sup>1</sup>, F. VILLAIN<sup>1</sup> and C. de RANGO<sup>1</sup>

<sup>1</sup>UPR 180 CNRS, <sup>2</sup>URA 1843 CNRS, Centre Pharmaceutique, Université Paris-Sud, 92290 Châtenay-Malabry, France

(Received August 8, 1994)

The first crystallographic example of a  $\beta$ -cyclodextrin monosubstituted at O6 by a bulky group possessing two terminal apolar side chains, *tert*-butoxycarbonyl-L-phenylalanyl-amino (Boc-L-Phe-NH), illustrates an unusual cyclodextrin host/guest organisation. The structure is a novel packing of monomer units. Two symmetry independent Boc-L-Phe-NH- $\beta$ -CD molecules are stacked parallel to the two-fold screw axis forming two independent alternate "endless screw head-to-tail" channels. Both apolar side chains are at the exterior of the intramolecular cavity and are fully enclosed within the channels: the phenyl ring of the amino residue lies above the parent macrocycle while the *tert*-butyl group is intermolecularly included within a neighbouring molecule. Water molecules located outside the monomeric cavities over 34 sites, all but one external to the channels, fill the intermolecular spaces and reinforce the cohesion of the structure.

## INTRODUCTION

Chemical modification of cyclodextrins via attachment of a biologically active molecule covalently bonded to the macrocycle *via* a hydroxyl group, has attracted much interest in recent years owing to the possible improvement of their properties in bio-organic chemistry, especially in the field of molecular recognition.<sup>1</sup>

The cyclodextrins (CDs) are cyclic oligosaccharides possessing an intramolecular cavity, which form stable complexes with a large variety of organic molecules. Examples of monosubstituted CD derivatives with functional groups have been reported.<sup>2</sup> They are of great interest for the development of new host-guest systems. It

is expected that the properties of such compounds will be strongly modified by the variation of the spatial relationship between the substituent group and the parent macrocycle, leading to changes in the molecular conformation and intermolecular interactions. Hence, to better understand the role of the non-covalent interactions in the conformational adaptation and to provide information about which chemical modifications are most appropriate, precise structural characterization by X-ray single crystal analysis is required. However, there are few crystallographic data available on monosubstituted  $\beta$ -CD derivatives; they concern mainly three classes of  $\beta$ -CD derivatives; all but one is substituted at the primary hydroxyl group (O6).

Firstly, short substituent groups grafted on  $\beta$ -CD do not affect significantly either the molecular conformation or the herringbone-type packing of the basic monomer  $\beta$ -CD hydrate isomorphous structure. Examples are provided with amino, azido<sup>3</sup> and iodo<sup>4</sup> at O6 or hydroxypropyl<sup>5</sup> at O2. In this last case, the substituent group is enclosed within the cavity of the adjacent molecule related by a two-fold screw axis.

Secondly, the monosubstituted  $\beta$ -CD derivatives with a relatively large hydrophobic group exhibit a tendency to pack in polymeric column-type structures, with the substituent group inserted within the cavity of the adjacent molecule in the column. The molecules are arranged, as monomeric units, in a structure of endless head-to-tail cylinder form. Although the association of successive molecules within a column are very similar, the overall packing depends strongly on the type of substituents. Surprisingly, isomorphous structures are observed for such chemically divergent groups as the *tert*-butylthio<sup>6</sup> or the 1,6 diamino hexyl moiety<sup>7</sup>. In contrast,

\*To whom correspondence should be addressed.

with hydrophobic substituents possessing aromatic moieties, the columns are formed and packed differently for close chemical entities such as phenylthio and phenylsulphanyl.<sup>8</sup> These monosubstituted  $\beta$ -CDs which act simultaneously as a host (CD moiety) and as a guest (hydrophobic substituent) are of interest as they provide models for systems having spacer arms exterior to the cavity of the parent macrocycle, and which may carry bio-functional systems.

Thirdly, the  $\beta$ -cyclodextrin monosubstituted with a bioactive bulky hydrophobic group, the cyclic dipeptide L-histidyl-L-leucine, adopts an unusual conformation with respect to those previously reported<sup>9</sup>: the hydrophobic terminal leucine side chain is now included within the cavity of the parent macrocycle. Nevertheless, the structure is again characterized by a similar molecular arrangement of the head-to-tail cylinder form, although in a novel packing mode. The tendency of the formation of auto-inclusion complex, observed for this dipeptido substrate, should be a more general feature of peptido or aromatic amino monosubstituted  $\beta$ -CD derivatives as it has been determined in aqueous solution by NMR studies<sup>10,11</sup> and supported by molecular graphics analysis, especially in the case of L- and D-phenylalanyl-amino- $\beta$ -CD derivatives.<sup>12</sup>

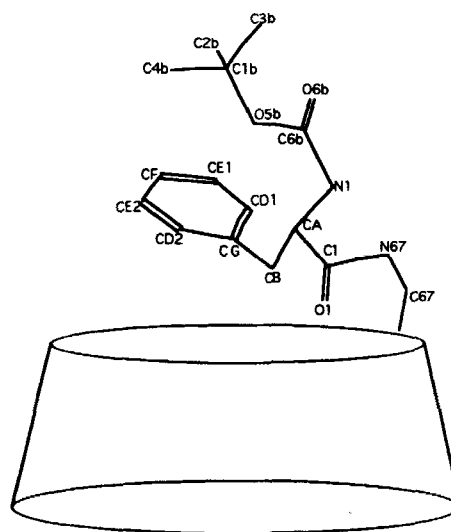
These structural investigations revealed that self-aggregation of the monosubstituted  $\beta$ -CD derivatives is pronounced and can accommodate differently the spatial insertion of a variety of substituents with respect to the parent macrocycle and to the molecular stack. Hence, structural elucidation of the molecular interactions which contribute to the optimal conformational adaptation of the functional group should lead to suitable selection of substituents favorable for molecular recognition by biological receptors.

We report here the first example of a crystalline form of a  $\beta$ -CD monosubstituted with a bulky group possessing two apolar terminal side chains. The *tert*-butoxycarbonyl-L-phenylalanyl-amino (Boc-L-Phe-NH) was chosen since the aromatic moiety of L-Phe and the *tert*-butyl group are considered as favorable entities for the formation of either intramolecular or intermolecular inclusion complexes. Competition between these two opposite tendencies will cause structural changes in the self aggregation of these classes of monosubstituted  $\beta$ -CD derivatives, pointing out the role of different apolar groups in this molecular recognition process.

## EXPERIMENTAL

### Preparation of 6<sup>A</sup>-Boc-L-Phenylalanyl-amino-6<sup>A</sup>-Deoxy- $\beta$ -CD

The title compound (Boc-L-Phe-NH- $\beta$ -CD) was synthesized by procedures previously reported<sup>9</sup> and fully char-



Scheme 1

acterized by proton NMR. Purification was achieved by recrystallisation from water at pH 8–9. Colourless crystals were grown by slow evaporation.

### X-Ray structural analysis

Single crystals of Boc-L-Phe-NH- $\beta$ -CD were sealed, in the presence of the mother liquor, in thin glass capillaries and then mounted on an Enraf-Nonius CAD-4 diffractometer. Cell constants were determined from setting angles of 25 reflections in the range  $9^\circ < \theta < 26^\circ$ . At scattering angles  $2\theta > 67^\circ$ , 50% diffracting planes had measurable intensity, but at  $2\theta > 90^\circ$  only very few had detectable intensity. Crystallographic data is summarized in Table 1.

The structure was solved straightforwardly by using the AMoRe package<sup>13</sup> which consists of the same steps of rotation function, translation function and rigid body refinement as conventional molecular replacement (MR) methods. Its main advantage is the high degree of automation; for example, when several molecules need to be found within the asymmetric unit, the information coming from already located molecules is automatically incorporated into the procedure. Furthermore, several search criteria are used simultaneously and a much larger portion of six-dimensional space than conventional MR methods is sampled by using fast and accurate algorithms. To improve the speed, the main programs of the package do not use atomic coordinates but Fourier coefficients.

The potential orientations are selected according to the correlation coefficient between observed and calculated truncated Patterson functions. A large number of retained orientations are then used to compute translation functions. First, a selection of peaks is made by computing the centered overlap of observed and calculated Patterson functions which is computed from the ob-

**Table 1** Crystallographic data collection and structure refinement

Formula	C <sub>56</sub> O <sub>37</sub> H <sub>88</sub> N <sub>2</sub>
Crystal size	0.4 × 0.4 × 0.3 mm
<b>Determination of unit cell</b>	
Radiation	Cu (λ = 1.54184 Å)
Space Group	P2 <sub>1</sub>
a(Å)	15.074(1)
b(Å)	18.637(2)
c(Å)	31.358(4)
β (°)	95.89(1)
V (Å <sup>3</sup> )	8763(1)
Z	4
<b>Intensity-data collection</b>	
θ range (°)	3–45
Maximum decay (%)	11.5
Unique reflections	7766
Reflections kept for refinement (I > 3σ(I))	4025
<b>Absorption correction</b>	
Correction method	Empirical (DIFABS) <sup>21</sup>
Minimum correction factor	0.5740
Average correction factor	0.9480
Maximum correction factor	1.6160
<b>Structure refinement</b>	
Minimized function	Σw( F <sub>o</sub> l -  F <sub>c</sub> l ) <sup>2</sup>
Weighting scheme	w = 3.522/(σ <sup>2</sup> (F) + 0.00343F <sup>2</sup> )
Maximum shift/e.s.d	1.7
R	0.12
R <sub>w</sub>	0.13
S	1.27

served, I<sub>obs</sub>(h), and calculated, I<sub>calc</sub>(h;R,t), intensities, where R and t represent the three rotation and translation parameters, respectively. The output is however a full correlation function Corr(F) defined in terms of amplitudes, F<sub>obs</sub>(h) and F<sub>calc</sub>(h;R,t), and calculated for the top peaks of the overlap function. The final list, sorted in descending order of correlation, includes also the R-factor. Finally the (R,t) parameters are refined by a fast rigid body refinement procedure for all retained positions.

The search object was a model structure of β-CD minus the primary hydroxyl groups (70 non-H atoms). Two independent molecules were located within the asymmetric unit cell. The correct solution corresponded to the 4th and the 6th peaks of the rotation function. Final Corr(F) and R-factors were 0.59 and 0.45, respectively, indicating a good fit of the molecular structure (consisting of 190 non H-atoms and a number of water molecules) with the model.

The positions of the Boc-L-Phe-NH group and of the primary hydroxyl groups of both molecules were revealed by Fourier syntheses. One fully and 33 partially occupied water sites were located in the asymmetric unit cell. The refinement was carried out using three block matrices in the least-squares minimization of Σw(ΔF)<sup>2</sup>. Due to the large number of parameters to be refined, only isotropic temperature factors were given to all atoms; H atoms bonded to C atoms were introduced in

ideal positions and allowed to ride on covalently bonded atoms. Stereochemical restraints were needed to handle the convergence refinement. The occupancy factors of water sites were estimated approximately from the height of the electron density and not refined. As a consequence, the total number of water molecules of crystallisation could not be determined with accuracy. In the final difference Fourier map there was no residual peak higher than 0.4eÅ<sup>-3</sup>. For molecule B, the atoms of G3, G4, G5 residues and of the substituent group show higher thermal motion than the related atoms of molecule A, though no disorder could be observed. Final atomic coordinates and thermal parameters of the non H atoms are given in Table 2.

All calculations were performed with the SHELX-76 package.<sup>14</sup> Analysis of the difference Fourier maps was carried out using the program FRODO<sup>15</sup> implemented on an Evans and Sutherland PS 330 Graphics Station. Molecular graphics studies have been performed using the SYBYL program package.<sup>16</sup>

## DISCUSSION

The crystal structure consists of two independent Boc-L-Phe-NH-β-CD molecules (Fig. 1) arranged, as monomeric units, in a novel packing of screw head-to-tail channel form. The substituent groups are fully enclosed within the channels with both apolar side chains at the exterior of the cavity of the parent macrocycle. The aromatic moiety is embedded between its own and an adjacent molecule (primary and secondary hydroxyl groups sides, respectively) while the *tert*-butyl group is intermolecularly included. The Boc-L-Phe-NH-β-CD molecular stacks leave large interstitial spaces, filled by water molecules.

### Arrangement of Boc-L-Phe-NH-β-CD molecules

The overall packing of the structure arises from the arrangement of the Boc-L-Phe-NH-β-CD molecules side by side giving rise to the formation of layers. The A and B independent molecules are alternately stacked along the c axis with the pseudo seven-fold axis of the macrocycle almost parallel to the b axis (9°) and the primary hydroxyl groups facing up (Molecule B) and down (Molecule A). Adjacent layers are related by the perpendicular screw two-fold b axis such that two symmetry related molecules (AA' or BB') are on top of each other. They are associated by their primary and secondary faces to form alternate screw head-to-tail channels (Cht) along the b axis (Fig. 2).

The resulting two antiparallel channels, ChtA and ChtB, each containing only the independent molecules A, or B, are not linear. The successive molecules in a channel show a lateral displacement on the ac plane, evaluated at 2.3 and 2.6 Å, from projections of centers of gravity

**Table 2** Fractional coordinates ( $\times 10^3$ ) and isotropic or equivalent thermal parameters ( $\times 10^2$ ) of the atoms

	<i>x</i>	<i>y</i>	<i>z</i>	<i>U(iso/eq)</i>	<i>x</i>	<i>y</i>	<i>z</i>	<i>U(iso/eq)</i>	
O(41A)	50 (1)	3 (0)	645 (1)	5 (1)	C(27A)	188 (2)	21 (2)	690 (1)	6 (1)
C(11A)	-213 (2)	34 (1)	611 (1)	7 (1)	C(37A)	242 (2)	30 (1)	651 (1)	5 (1)
C(21A)	-168 (2)	92 (1)	640 (1)	6 (1)	C(47A)	269 (2)	-39 (2)	633 (1)	7 (1)
C(31A)	-66 (2)	85 (1)	639 (1)	6 (1)	C(57A)	189 (2)	-88 (1)	622 (1)	4 (1)
C(41A)	-42 (2)	9 (1)	653 (1)	5 (1)	C(67A)	214 (2)	-163 (1)	608 (1)	5 (1)
C(51A)	-94 (2)	-46 (1)	624 (1)	4 (1)	O(27A)	153 (2)	86 (1)	703 (1)	9 (1)
C(61A)	-72 (2)	-122 (1)	641 (1)	8 (1)	O(37A)	319 (1)	71 (1)	665 (1)	7 (1)
O(21A)	-197 (2)	161 (1)	625 (1)	9 (1)	O(57A)	147 (1)	-96 (1)	659 (1)	6 (1)
O(31A)	-21 (1)	137 (1)	667 (1)	7 (1)	N(67A)	133 (1)	-201 (1)	592 (1)	4 (1)
O(51A)	-188 (1)	-35 (1)	626 (1)	5 (1)	C(1A)	105 (2)	-203 (2)	552 (1)	6 (1)
O(61A)	-121 (2)	-171 (1)	614 (1)	8 (1)	O(1A)	137 (2)	-162 (1)	527 (1)	9 (1)
O(42A)	-200 (1)	45 (1)	568 (1)	6 (1)	C(AA)	26 (2)	-246 (1)	532 (1)	4 (1)
C(12A)	-329 (2)	50 (1)	447 (1)	6 (1)	C(BA)	-41 (2)	-192 (2)	510 (1)	6 (1)
C(22A)	-327 (2)	120 (1)	472 (1)	6 (1)	C(GA)	-118 (2)	-232 (2)	483 (1)	7 (1)
C(32A)	-261 (2)	115 (1)	510 (1)	4 (1)	C(D1A)	-197 (2)	-253 (2)	500 (1)	7 (1)
C(42A)	-272 (2)	49 (1)	536 (1)	6 (1)	C(E1A)	-266 (2)	-290 (2)	477 (1)	9 (1)
C(52A)	-273 (2)	-18 (1)	508 (1)	4 (1)	C(FA)	-259 (3)	-309 (2)	435 (1)	10 (1)
C(62A)	-290 (2)	-87 (1)	531 (1)	6 (1)	C(E2A)	-180 (2)	-294 (2)	417 (1)	10 (1)
O(22A)	-309 (1)	177 (1)	444 (1)	7 (1)	C(D2A)	-109 (2)	-257 (2)	442 (1)	7 (1)
O(32A)	-272 (1)	176 (1)	536 (1)	7 (1)	N(2A)	-16 (2)	-277 (1)	568 (1)	6 (1)
O(52A)	-341 (1)	-8 (1)	474 (1)	4 (1)	C(6bA)	-46 (2)	-343 (1)	566 (1)	7 (1)
O(62A)	-369 (1)	-82 (1)	554 (1)	8 (1)	O(6bA)	-93 (2)	-372 (1)	591 (1)	8 (1)
O(43A)	-249 (1)	43 (1)	426 (1)	6 (1)	O(5bA)	-22 (1)	-386 (1)	533 (1)	5 (1)
C(13A)	-164 (2)	-18 (1)	312 (1)	5 (1)	C(1bA)	-53 (2)	-458 (1)	521 (1)	3 (1)
C(23A)	-205 (2)	55 (2)	313 (1)	8 (1)	C(2bA)	-155 (2)	-458 (2)	516 (1)	8 (1)
C(33A)	-207 (2)	79 (1)	359 (1)	6 (1)	C(3bA)	-12 (3)	-504 (2)	557 (1)	11 (1)
C(43A)	-259 (2)	24 (1)	383 (1)	5 (1)	C(4bA)	-13 (2)	-475 (2)	481 (1)	8 (1)
C(53A)	-223 (2)	-49 (1)	376 (1)	5 (1)	O(41B)	987 (1)	10 (1)	1137 (1)	6 (1)
C(63A)	-281 (2)	-106 (2)	393 (1)	8 (1)	C(11B)	1247 (2)	-20 (1)	1109 (1)	10 (1)
O(23A)	-150 (2)	107 (1)	291 (1)	8 (1)	C(21B)	1206 (2)	-76 (1)	1136 (1)	7 (1)
O(33A)	-238 (1)	151 (1)	364 (1)	6 (1)	C(31B)	1106 (2)	-70 (1)	1136 (1)	8 (1)
O(53A)	-219 (1)	-66 (1)	332 (1)	6 (1)	C(41B)	1079 (2)	6 (1)	1146 (1)	6 (1)
O(63A)	-371 (2)	-99 (1)	375 (1)	10 (1)	C(51B)	1127 (2)	60 (1)	1119 (1)	5 (1)
O(44A)	-76 (1)	-18 (1)	331 (1)	5 (1)	C(61B)	1114 (2)	136 (1)	1133 (1)	7 (1)
C(14A)	179 (2)	-75 (1)	306 (1)	5 (1)	O(21B)	1229 (2)	-147 (1)	1123 (1)	10 (1)
C(24A)	133 (2)	-16 (1)	278 (1)	7 (1)	O(31B)	1069 (2)	-116 (1)	1166 (1)	10 (1)
C(34A)	55 (2)	13 (1)	299 (1)	5 (1)	O(51B)	1220 (1)	49 (1)	1122 (1)	8 (1)
C(44A)	-7 (2)	-48 (1)	309 (1)	5 (1)	O(61B)	1140 (1)	183 (1)	1100 (1)	9 (1)
C(54A)	45 (2)	-105 (1)	334 (1)	4 (1)	O(42B)	1216 (1)	-35 (1)	1064 (1)	7 (1)
C(64A)	-15 (2)	-171 (1)	337 (1)	6 (1)	C(12B)	1322 (2)	-36 (1)	947 (1)	7 (1)
O(24A)	195 (1)	41 (1)	269 (1)	9 (1)	C(22B)	1321 (2)	-106 (2)	972 (1)	10 (1)
O(34A)	9 (1)	65 (1)	270 (1)	7 (1)	C(32B)	1259 (2)	-102 (1)	1008 (1)	7 (1)
O(54A)	118 (1)	-130 (1)	313 (1)	5 (1)	C(42B)	1281 (2)	-36 (1)	1036 (1)	6 (1)
O(64A)	36 (2)	-218 (1)	366 (1)	13 (1)	C(52B)	1284 (2)	29 (1)	1008 (1)	8 (1)
O(45A)	213 (1)	-41 (1)	345 (1)	6 (1)	C(62B)	1309 (2)	98 (2)	1032 (1)	10 (1)
C(15A)	439 (2)	-37 (1)	431 (1)	5 (1)	O(22B)	1299 (1)	-167 (1)	945 (1)	8 (1)
C(25A)	425 (2)	23 (1)	399 (1)	6 (1)	O(32B)	1267 (1)	-165 (1)	1034 (1)	7 (1)
C(35A)	328 (2)	27 (1)	381 (1)	7 (1)	O(52B)	1341 (1)	22 (1)	975 (1)	6 (1)
C(45A)	305 (2)	-46 (1)	360 (1)	4 (1)	O(62B)	1392 (2)	94 (1)	1056 (1)	10 (1)
C(55A)	324 (2)	-105 (1)	393 (1)	6 (1)	O(43B)	1235 (1)	-27 (1)	926 (1)	6 (1)
C(65A)	310 (2)	-180 (1)	375 (1)	6 (1)	C(13B)	1118 (2)	34 (1)	805 (1)	9 (1)
O(25A)	447 (1)	89 (1)	421 (1)	7 (1)	C(23B)	1160 (2)	-40 (2)	809 (1)	9 (1)
O(35A)	323 (1)	80 (1)	346 (1)	7 (1)	C(33B)	1174 (2)	-64 (1)	855 (1)	8 (1)
O(55A)	414 (1)	-102 (1)	412 (1)	5 (1)	C(43B)	1228 (2)	-9 (1)	883 (1)	8 (1)
O(65A)	361 (2)	-190 (1)	340 (1)	9 (1)	C(53B)	1187 (2)	65 (1)	877 (1)	7 (1)
O(46A)	386 (1)	-20 (1)	465 (1)	4 (1)	O(63B)	1247 (2)	127 (2)	896 (1)	11 (1)
C(16A)	404 (2)	-42 (1)	596 (1)	5 (1)	O(23B)	1105 (2)	-90 (1)	783 (1)	12 (1)
C(26A)	448 (2)	21 (1)	578 (1)	5 (1)	O(33B)	1212 (2)	-134 (1)	860 (1)	10 (1)
C(36A)	413 (2)	36 (1)	532 (1)	3 (1)	O(53B)	1171 (1)	83 (1)	832 (1)	9 (1)
C(46A)	425 (2)	-35 (1)	507 (1)	4 (1)	O(63B)	1332 (2)	122 (1)	879 (1)	14 (1)
C(56A)	383 (2)	-97 (1)	529 (1)	6 (1)	O(44B)	1034 (1)	29 (1)	822 (1)	8 (1)
C(66A)	400 (2)	-169 (2)	509 (1)	7 (1)	C(14B)	774 (2)	84 (2)	794 (1)	11 (1)
O(26A)	439 (1)	83 (1)	603 (1)	6 (1)	C(24B)	805 (2)	23 (2)	768 (1)	9 (1)
O(36A)	458 (1)	93 (1)	514 (1)	6 (1)	C(34B)	895 (2)	-3 (2)	788 (1)	8 (1)
O(56A)	421 (1)	-103 (1)	572 (1)	5 (1)	C(44B)	960 (2)	58 (1)	798 (1)	8 (1)
O(66A)	490 (2)	-184 (1)	510 (1)	8 (1)	C(54B)	919 (2)	116 (1)	820 (1)	6 (1)
O(47A)	313 (1)	-26 (1)	597 (1)	4 (1)	C(64B)	976 (2)	182 (1)	827 (1)	8 (1)
C(17A)	111 (2)	-31 (1)	675 (1)	7 (1)	O(24B)	744 (2)	-33 (1)	763 (1)	13 (1)
					O(34B)	932 (2)	-55 (1)	762 (1)	11 (1)
					O(54B)	836 (2)	140 (1)	799 (1)	12 (1)
					O(64B)	994 (2)	204 (1)	785 (1)	14 (1)

	x	y	z	U(iso/eq)		x	y	z	U(iso/eq)
O(45B)	754 (1)	52 (1)	834 (1)	8 (1)	W(B5)	391 (3)	868 (2)	833 (1)	10 (1)
C(15B)	549 (2)	60 (1)	910 (1)	7 (1)	W(B6)	412 (4)	294 (4)	43 (2)	7 (2)
C(25B)	541 (2)	4 (1)	877 (1)	7 (1)	W(B7)	344 (3)	491 (2)	776 (1)	11 (1)
C(35B)	633 (2)	-6 (1)	860 (1)	8 (1)	W(B8)	431 (4)	98 (3)	141 (2)	10 (2)
C(45B)	667 (2)	67 (2)	846 (1)	11 (1)	W(B9)	194 (5)	339 (4)	157 (2)	7 (2)
C(55B)	671 (2)	115 (2)	886 (1)	9 (1)	W(B10)	78 (3)	769 (2)	829 (1)	8 (1)
C(65B)	713 (3)	186 (2)	875 (1)	20 (2)	W(B11)	22 (3)	782 (3)	838 (1)	11 (2)
O(25B)	511 (2)	-61 (1)	893 (1)	11 (1)	W(B12)	279 (4)	289 (3)	106 (2)	11 (2)
O(35B)	619 (2)	-48 (1)	822 (1)	12 (1)	W(B13)	326 (5)	215 (4)	123 (2)	8 (2)
O(55B)	585 (2)	124 (1)	899 (1)	12 (1)	W(C1)	135 (2)	730 (1)	281 (1)	9 (1)
O(65B)	660 (2)	217 (2)	839 (1)	17 (1)	W(C2)	202 (2)	820 (2)	741 (1)	10 (1)
O(46B)	601 (1)	33 (1)	946 (1)	9 (1)	W(C3)	326 (5)	91 (4)	212 (2)	9 (3)
C(16B)	619 (2)	41 (1)	1079 (1)	9 (1)	W(D1)	393 (5)	891 (4)	247 (3)	11 (3)
C(26B)	575 (2)	-25 (1)	1058 (1)	7 (1)	W(D2)	466 (4)	925 (4)	160 (2)	11 (2)
C(36B)	594 (2)	-29 (1)	1013 (1)	9 (1)					
C(46B)	572 (2)	39 (1)	988 (1)	7 (1)					
C(56B)	614 (2)	102 (1)	1014 (1)	7 (1)					
C(66B)	587 (2)	173 (2)	994 (1)	9 (1)					
O(26B)	602 (2)	-86 (1)	1083 (1)	10 (1)					
O(36B)	549 (2)	-88 (1)	994 (1)	11 (1)					
O(56B)	590 (1)	102 (1)	1056 (1)	8 (1)					
O(66B)	493 (2)	180 (1)	997 (1)	11 (1)					
O(47B)	712 (1)	31 (1)	1083 (1)	7 (1)					
C(17B)	937 (2)	44 (1)	1166 (1)	10 (1)					
C(27B)	864 (2)	-5 (1)	1182 (1)	7 (1)					
C(37B)	801 (2)	-20 (1)	1143 (1)	8 (1)					
C(47B)	762 (2)	48 (1)	1122 (1)	7 (1)					
C(57B)	836 (2)	97 (1)	1111 (1)	6 (1)					
C(67B)	804 (2)	170 (1)	1097 (1)	8 (1)					
O(27B)	908 (1)	-71 (1)	1195 (1)	9 (1)					
O(37B)	726 (2)	-64 (1)	1151 (1)	11 (1)					
O(57B)	894 (1)	108 (1)	1150 (1)	7 (1)					
N(67B)	873 (2)	216 (1)	1083 (1)	6 (1)					
C(1B)	878 (2)	230 (2)	1042 (1)	8 (1)					
O(1B)	821 (2)	210 (1)	1014 (1)	11 (1)					
C(AB)	956 (2)	268 (2)	1024 (1)	7 (1)					
C(BB)	1003 (3)	210 (2)	999 (1)	11 (1)					
C(GB)	1071 (2)	251 (2)	974 (1)	6 (1)					
C(D1B)	1160 (2)	257 (2)	991 (1)	10 (1)					
C(E1B)	1226 (2)	288 (2)	968 (1)	11 (1)					
C(FB)	1199 (3)	316 (2)	927 (1)	11 (1)					
C(E2B)	1112 (2)	311 (2)	910 (1)	12 (1)					
C(D2B)	1048 (2)	283 (2)	935 (1)	10 (1)					
N(1B)	1016 (2)	293 (1)	1063 (1)	6 (1)					
C(6bB)	1059 (2)	355 (2)	1064 (1)	10 (1)					
O(6bB)	1125 (2)	375 (1)	1090 (1)	11 (1)					
O(5bB)	1024 (1)	401 (1)	1032 (1)	5 (1)					
C(1bB)	1059 (2)	473 (1)	1027 (1)	5 (1)					
C(2bB)	1156 (2)	475 (2)	1022 (1)	10 (1)					
C(3bB)	1038 (3)	520 (2)	1065 (1)	10 (1)					
C(4bB)	1005 (2)	502 (2)	987 (1)	11 (1)					
W(A1)	466 (1)	273 (1)	625 (1)	8 (1)					
W(A2)	86 (2)	739 (1)	673 (1)	8 (1)					
W(A3)	471 (2)	712 (1)	448 (1)	8 (1)					
W(A4)	238 (3)	681 (2)	778 (1)	10 (1)					
W(A5)	163 (2)	796 (2)	444 (1)	9 (1)					
W(A6)	481 (3)	730 (2)	593 (1)	9 (1)					
W(A7)	323 (3)	687 (2)	298 (1)	9 (1)					
W(A8)	208 (2)	182 (2)	358 (1)	10 (1)					
W(A9)	87 (3)	207 (2)	289 (1)	10 (1)					
W(A10)	372 (3)	208 (2)	690 (1)	9 (1)					
W(A11)	225 (5)	279 (4)	695 (3)	10 (3)					
W(A12)	434 (3)	444 (2)	703 (1)	9 (1)					
W(A13)	414 (4)	618 (3)	348 (2)	10 (2)					
W(A14)	392 (4)	686 (3)	688 (2)	8 (2)					
W(A15)	305 (3)	321 (2)	380 (1)	9 (1)					
W(A16)	384 (6)	372 (5)	358 (3)	11 (3)					
W(B1)	428 (3)	246 (2)	924 (1)	9 (1)					
W(B2)	160 (3)	299 (2)	783 (1)	10 (1)					
W(B3)	220 (2)	811 (2)	215 (1)	8 (1)					
W(B4)	435 (3)	754 (2)	907 (1)	8 (1)					

of O4 atoms, for AA' and BB', respectively. The dihedral angle between their O4 least-squares planes of about 17° is considerably smaller than the corresponding dihedral angle (-45°) observed in all previously reported column-type structures of monosubstituted  $\beta$ -CD derivatives. Both independent ChtA and ChtB are packed along the translation **a** axis forming sheets parallel to the **ab** plane (Fig. 3); there are, then, two "antiparallel" sheets SChtA and SChtB alternately stacked along the **c** axis, respectively at the levels  $z = 1/2$  and  $z = 0$ .

Only a few intermolecular short contacts are observed (Table 3). Between primary and secondary hydroxyl groups of two consecutive monomers within the ChtA, only one hydrogen bond contact exists (O64A-O31A'), the shortest similar intermolecular contact in ChtB being somewhat larger (O65B-O21B', 3.21 Å). Between ChtA and ChtB, no intermolecular short contacts occur. This arises from the arrangement of the monomers within layers containing two independent rows of A or B molecules (Fig. 4). The rows are, each, probably hydrogen bonded along the translation **a** axis via two primary hydroxyls in the sole intralayer intermolecular interaction (O62-O66'), but they are separated by two independent interstitial spaces filled by water molecules in different arrangements.

### Macrocyclic ring conformation

The monosubstitution of the  $\beta$ -CD molecules does not affect significantly the macrocycle conformation. Both symmetry independent Boc-L-Phe-NH- $\beta$ -CD molecules occur in the ordinarily observed macrocyclic conformation with average bond distances and angles in the normal range and there are no critical differences between the two independent units (Table 4). The distances of the O4 to their least-squares plane vary between -0.30 and 0.40 Å and the geometry of the O4 heptagons are approximately regular with radii in the range 4.92-5.13 Å, for both molecules.

An approximate two-fold screw axis relating the two independent monomers is nearly parallel to the **c**-axis

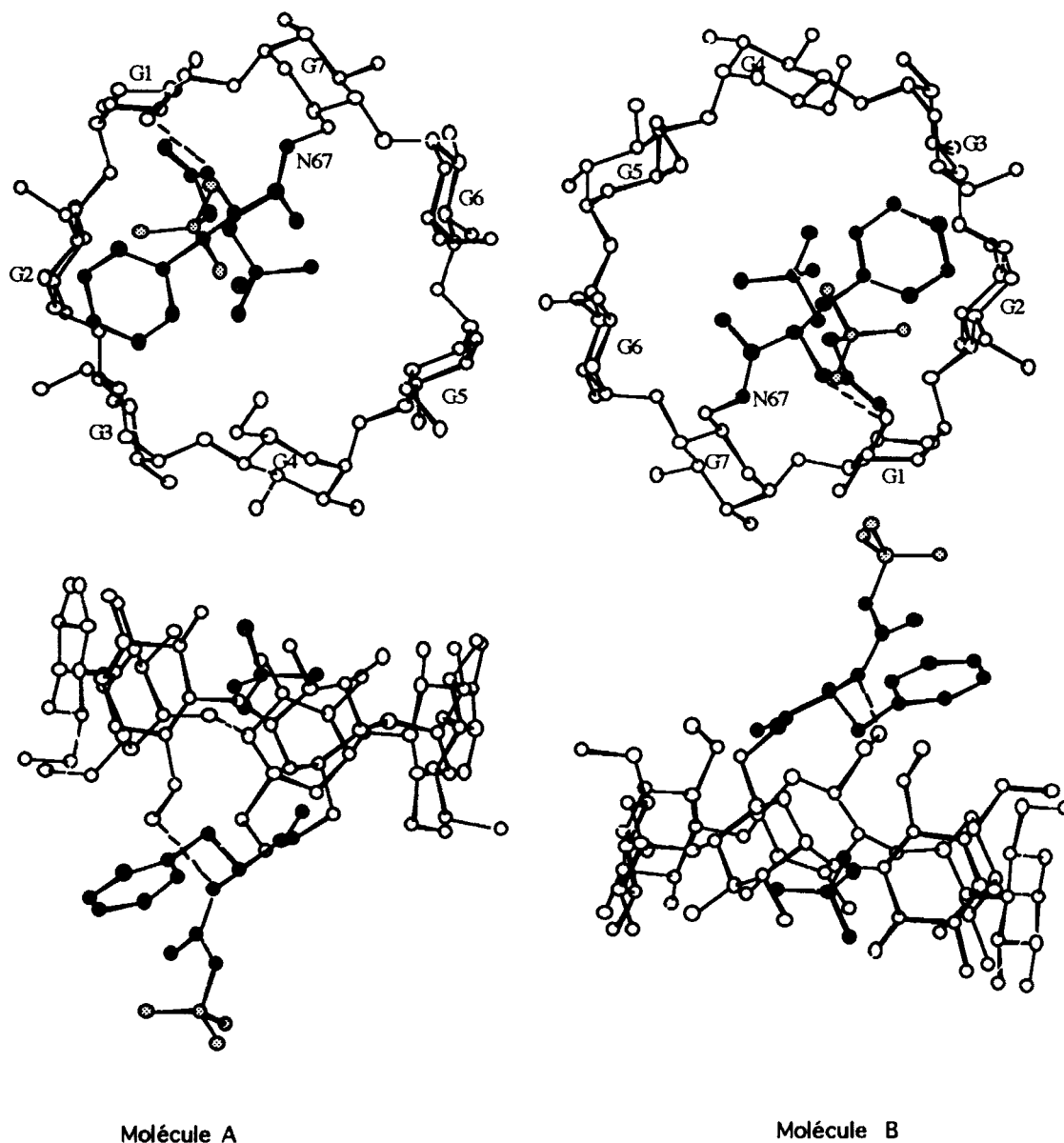


**Figure 1** Molecular structure of A and B molecules. Substituents groups are shown by filled circles. The *tert*-butyl of the adjacent molecule, intermolecularly included in the hydrophobic cavity, is depicted in grey. The intramolecular short contacts (O61-N1) are indicated in ---.

and there exists a close correlation as well between tilt angles as between torsion angles of the pseudo related glucopyranose residues  $G_nA$  and  $G_nB$ , numerated 1 through 7,  $G7$  designing the substituted residue. In both molecules the tilt angle of an adjacent residue of  $G7$  is larger than usually observed ( $21.9$  and  $25.9^\circ$ , respectively for molecules A and B). The tilt angles of the remaining residues range from  $6.0$  to  $9.9^\circ$ , except for  $G3$  ( $16.1$  and  $15.4^\circ$ , respectively). The torsion angles concerning the orientation of the  $C(6)-O(6)$  bonds show the same relative conformation for all but one ( $G4$ ) pseudo related residues: *gauche-trans* for  $G1A$ ,  $G1B$  and  $G4A$ , (implying that the  $C6-O6$  bonds point towards the molecular axis), and *gauche-gauche* for the remaining residues, including  $G4B$ .

The rigid conformation of both macrocycles is stabilized, as is usually observed for native  $\beta$ -CD molecules, by a ring of intramolecular hydrogen bonds,<sup>17</sup> with 13 distances  $O(2)n-O(3)n+1$  within the range  $2.68$ – $3.03\text{\AA}$  and only one somewhat larger ( $O25B-O36B$ ,  $3.20\text{\AA}$ ).

#### Water molecules

All the sites of water molecules are located outside of the cavities of the monomers and, except for one (WA5), exterior to the channels. There no doubt exist frequent interactions between hydroxyl groups and water molecules. As shown in Figure 5, all the independent primary hydroxyl groups, the two linkage amide nitrogen atoms and most of the secondary hydroxyls are at hydrogen bond distances from water molecules.

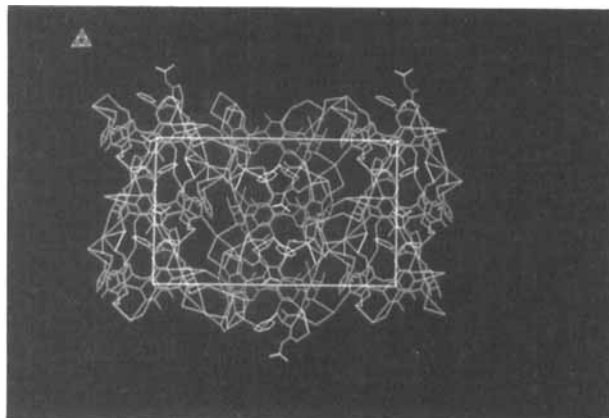


**Figure 2** Projection of the structure on the *bc* plane (*c* horizontal) showing the stacking of the two independent head-to-tail channels, ChtA (blue,  $z = 1/2$ ) and ChtB (red,  $z = 0$ ), along the *c* axis and illustrating the role of the water molecules (green). (See Color Plate I.)

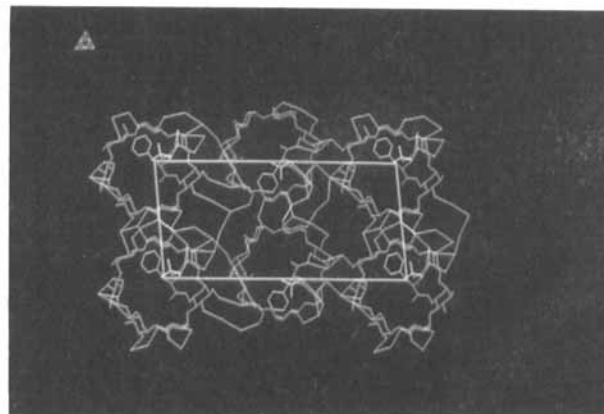


**Figure 4** Section of the structure parallel to the *ac* plane (*c* horizontal) showing the stacking of the rows of molecules A (blue) and B (red) within a layer. Water molecules are indicated in green. (See Color Plate III.)

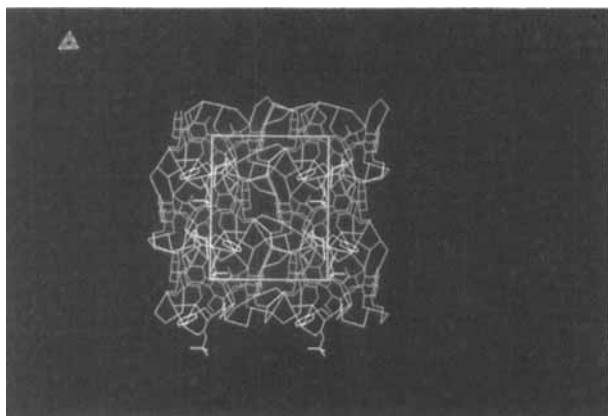


**Figure 3** Section of the structure parallel to the *ab* plane (*a* horizontal) representing one sheet of parallel channels (ChtA) and showing the role of the water molecules within the sheet (SChtA). (See Color Plate II.)

**Table 3** Intra- and Intermolecular Short Contacts

Atom1	Atom2	Distance in Å
O64A	O31A(a)	2.89(2)
O62A	O66A(b)	3.06(3)
O62B	O56B(c)	2.99(3)
O62B	O66B(c)	2.97(3)
O1B	O32B(d)	3.01(3)
O61A	N1A	2.98(3)
O61B	N1B	2.94(3)
O64A	WA5(e)	2.97(3)
O1A	WA5(e)	2.76(3)
WA5	O32A(f)	2.80(3)

Symmetry operation:

(a):  $-x, y - 1/2, -z + 1$

(b):  $x - 1, y, z$

(c):  $x + 1, y, z$

(d):  $-x + 2, y + 1/2, -z + 2$

(e):  $x, y - 1, z$

(f):  $-x, y - 1/2, -z$

A detailed description of the hydrogen bonding scheme involving the water molecules requires the experimental determination of the H-positions and an accurate estimation of the occupancy factors, not available from the present X-ray data. The partial occupancy of all

**Table 4** Geometrical data for A and B Boc-L-Phe-NH- $\beta$ -CD molecules

Residue	Tilt( $^{\circ}$ )		O4 distance from O4 plane(Å)		O5-C5-C6-O6 torsion ( $^{\circ}$ )	
	A	B	A	B	A	B
G1	6.5	8.9	-0.253	-0.294	62	72
G2	6.0	7.9	-0.140	0.178	-68	-69
G3	16.1	15.4	0.265	0.215	-68	-67
G4	9.7	7.7	-0.297	-0.252	67	-68
G5	6.9	5.6	-0.135	-0.134	-66	-63
G6	21.9	25.9	0.398	0.345	-63	-57
G7	8.7	9.9	-0.117	-0.059	-	-

The tilt angle is defined by the dihedral angle between the O(4) plane and the least-squares plane through O(4( $n - 1$ )), C(1 $n$ ), C(4 $n$ ), O(4 $n$ ) of each residue.

but one water sites may arise from positional disorder which cannot be resolved at the experimental resolution. Only three cases of two mutually exclusive sites are observed, the sum of occupancy factors being equal or less than 1. It is likely that the total amount of solvent is underestimated. Nevertheless, from an analysis of the short contacts, with a O...O distance cut-off criterion of 3.2Å, similar characteristics between water molecule arrangements around the A and B molecules are distinguishable.

A striking feature is that almost all of the water molecules are in short contacts with O-atoms of only one of the two independent molecules A and B (WA1 - WA16 and WB1 - WB13 for molecules A and B, respectively). They are located in such a way as to form through the two-fold screw *b* axis two independent systems, each surrounding one of the channels, ChtA or ChtB. Among the five additional water molecules, three (WC) are involved in bridges between molecules A and B, and two (WD) are bonded only to other water molecules.

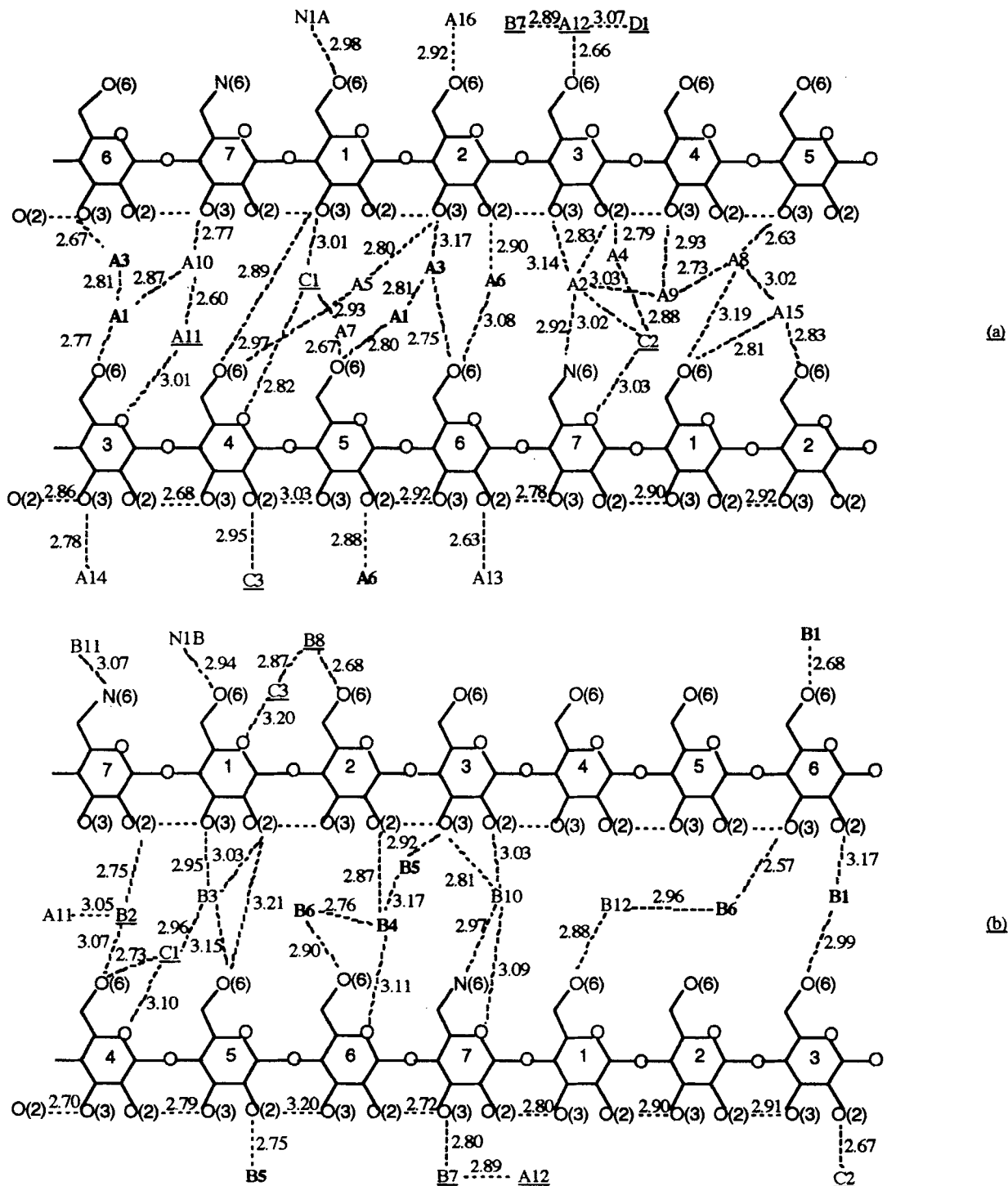


**Figure 5** Schematic representation of short contacts involving water molecules, primary and secondary hydroxyl groups of two successive molecules within channels ChtA (a) and ChtB (b). Water molecules involved in the cohesion of the sheets are indicated in bold, those serving to form intermolecular bridges between ChtA and ChtB are underlined.

Most of the water molecules are situated in the inter-layer spaces, forming rings at the level of the primary and secondary hydroxyl faces of two symmetry related molecules, AA' or BB'. They are probably engaged in hydrogen bonds stabilizing the association of the successive molecules within a channel. Figure 6 illustrates how

the cage formed by the AA' association is surrounded by water molecules: 12 out of the 16 WA and two WC may be involved in hydrogen bonds either as singlets or as doublets. All the primary and the O3 secondary hydroxyls show short contacts with water molecules (Fig. 5a). In the BB' association, this pattern is slightly different,

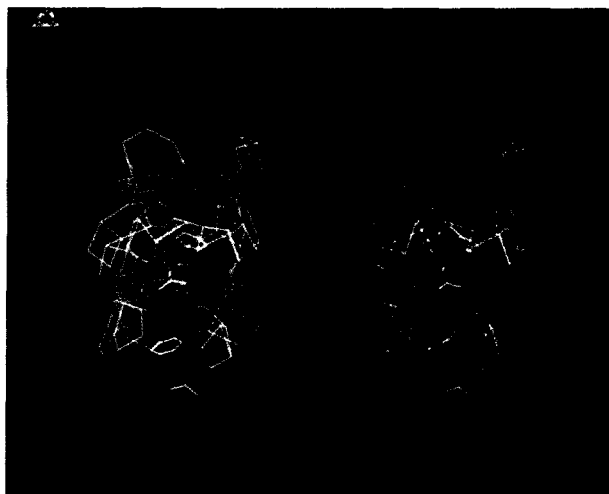


**Figure 6** Stereoview of the AA' molecular association with the cortege of water molecules (green) surrounding the cage (substituent group: backbone of the main chain, red; phenyl ring, purple; methyl C-atoms, yellow). (See Color Plate IV.)

mainly because one primary hydroxyl is not connected by water molecules to the secondary hydroxyls of face to face residues (Fig. 5b).

Moreover, several WA or WB, are situated between parallel channels (Fig. 3), being involved in bridges between monomers related by translation along the *a* axis, either at the primary-primary (one singlet for both SChA and SChB) or at the secondary-secondary hydroxyl levels (two singlets for SChA or one singlet and one doublet for SChB). All these water molecules being also involved in the hydration scheme surrounding the cages formed by the AA' or BB' association, they probably reinforce the stability within the sheets along the *ab* plane.

In the absence of intermolecular short contacts between the A and B molecules, the cohesion between antiparallel sheets SChA and SChB arises undoubtedly from interactions involving water molecules situated in the two intralayer interstitial spaces which separate the independent rows. On one side, two WC singlets, on the other side, one WC singlet, one WC-WB doublet and two WA-WB doublets serve to form bridges between molecules A and B lying in adjacent antiparallel channels (Fig. 2 and 4).

Thus, the water molecules form a layer of hydration around ChtA and ChtB (Fig. 7) and play an important role in the cohesion of the structure: they participate simultaneously to the association of successive molecules AA' or BB' within a channel and to the stability within the sheets, along the *ab* plane; also they ensure the stability of the packing of antiparallel sheets, along the *c* axis.

#### Conformation and spatial insertion of Boc-L-Phe-NH groups

The substituent groups (Fig. 8) are inserted within the cages formed in the channels from the association of the



**Figure 7** Projection of the structure parallel along the *b* axis (*c* horizontal) showing the packing of the channels, ChtA (blue) and ChtB (red), surrounded by the cortege of water molecules (green). (See Color Plate V.)

successive Boc-L-Phe-NH- $\beta$ -CD molecules (AA' or BB'). They adopt quite similar conformation in both molecules, without significant differences in their spatial arrangements as indicated by the torsion angles (Table 5) which do not differ by larger than  $15^\circ$ . The L-Phe amino acid is positioned above the parent macrocycle A or B, deviated towards the G1 to G3 residues side, while the Boc is directed towards the cavity of the molecule A' or B'. As a consequence, the substituents are encapsulated within the channels and do not point away to the aqueous environment (Fig. 6).

The Boc-L-Phe-NH groups show a torsion angle corresponding to a *gauche-trans* conformation with respect to the glucopyranose residue. The main chain skeleton can be described by the two pseudo-peptide planes (C67, N67, C1, O1, CA) and (CA, N1, C6b, O6b, O5b) which

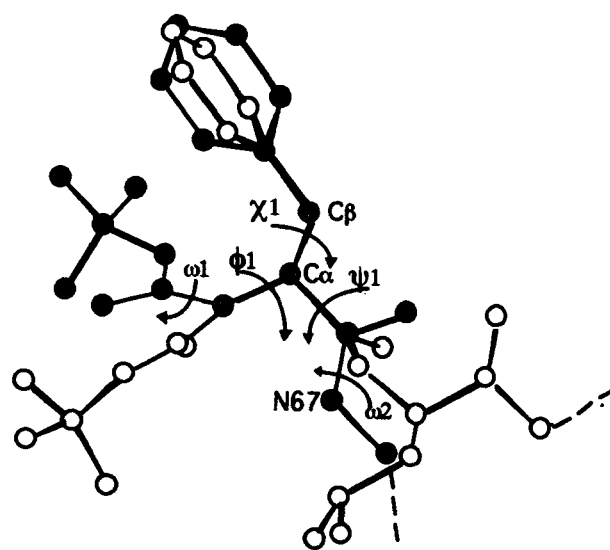


**Figure 8** Molecular conformation of the Boc-L-Phe-NH (molecule A, filled circles) compared with the open conformation (open circles) as observed in Boc-L-Phe-D-Leu-OMe structure<sup>19</sup> (relative positions around the L-Phe C $\alpha$ ).

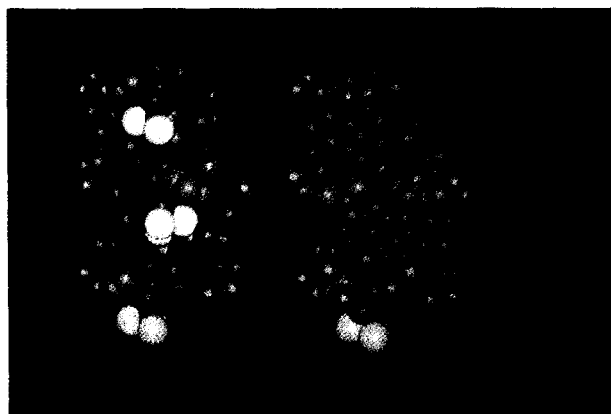
**Table 5** Selected torsion angles for Boc-L-Phe-NH- group in molecules A and B

	Atom1	Atom2	Atom3	Atom4	Angle in (°) Mol A	Angle in (°) Mol B
	O57	C57	C67	N67	70	67
$\phi_2$	C1	N67	C67	C57	94	105
$\omega_2$	CA	C1	N67	C67	175	-169
$\psi_1$	N1	CA	C1	N67	6	-6
$\chi_1$	N1	CA	CB	CG	-74	-76
$\phi_1$	C6b	N1	CA	C1	-139	-143
$\chi_2$	CA	CB	CG	CD1	90	96
$\omega_1$	O5b	C6b	N1	CA	10	16
	N1	C6b	O5b	C1b	-173	178
	C6b	O5b	C1b	C2b	53	56
	C6b	O5b	C1b	C3b	-68.4	-67
	C6b	O5b	C1b	C4b	175	177

form a dihedral angle of  $126^\circ$  and  $136^\circ$  for molecules A and B, respectively (mean planar deviations,  $0.06\text{\AA}$ ). The L-Phe backbone is oriented towards the molecular axis owing to the expected *trans* pseudo-peptide bond ( $\omega_2 = 175$  or  $-170^\circ$ ), but the CA-N1 bond is directed towards the G1 residue. The most interesting conformational feature is that the Boc group is folded back on the L-Phe side chain, as indicated by the  $\phi_1$  and  $\omega_1$  angles.

This conformation is expected when Boc is bound to a proline<sup>18</sup> but is considerably less extended than usually observed in peptide structures when Boc is attached to L-Phe,<sup>19</sup> the corresponding  $\phi_1$  and  $\omega_1$  angles being of about  $-80^\circ$  and  $170^\circ$ , respectively, as illustrated in Figure 8. This conformational adaptation should be related to the lateral orientation of the CA-N1 bond which gives rise to steric constraints for the position of the Boc relative to the parent macrocycle. The observed  $\phi_1$  angle and the *cis* pseudo-peptide bond ( $\omega_1 = 11$  or  $17^\circ$ ) direct the C6b-O5b bond towards the cavity of the adjacent molecule (A' or B'). Hence, this non extended conformation provides a suitable fit of the main chain skeleton for the intermolecular inclusion of the *tert*-butyl group and for the encapsulation of the aromatic ring within the cages, as shown in Figure 9.

The *tert*-butyl groups enter the cavity of the A' and B' molecules from the secondary hydroxyl groups side and they are deeply included within the host molecule, the C1b atoms and the methyl C-atoms being at distances less than  $1.0\text{\AA}$  above the macrocycle O4 least-squares plane. They occupy similar relative positions in the central part of the cavities of the A' and B' host molecules, with the projections of the C1b atoms on the macrocycle O4 heptagon not deviated from the center of gravity. One of the distances between the methyl C-atoms and the O-atom of the Boc-carboxyl ( $2.91\text{\AA}$ ) is shorter than usually observed in the Boc-L-Phe peptide structures (about  $3.03\text{\AA}$ ). This partly explains the absence of thermal disorder for the methyl C-atoms. Moreover close contacts are observed between the atoms of the host macrocycle

**Figure 9** Space filling model of the association of molecules A and A' within ChtA. (See Color Plate VI.)

and the methyl C-atoms, especially with the O41, O42, O44 and O46 anomeric atoms (mean values  $3.78\text{\AA}$ ).

The *gauche* orientation of the L-Phe side-chain is the most frequently observed conformation for this residue in peptides and proteins.<sup>20</sup> The phenyl ring forms a dihedral angle of  $37.7^\circ$  with the O6 least-squares plane of molecule A and of  $26.1^\circ$  with the O2/O3 least-squares plane of molecule A' ( $35.5^\circ$  and  $29.6^\circ$ , respectively, for molecules B and B'). Many close contacts are observed either with atoms of the parent macrocycle A or B (residues G1 to G4) or with those of molecule A' or B' (residues G6, G7 and G1), showing strong steric constraints on the position of the L-Phe inside the cages (mean values  $3.89$  and  $3.73\text{\AA}$  for C..C and C..O distances smaller than  $4.2$  and  $4.0\text{\AA}$ , respectively).

All the observed close contacts indicate a tight packing of the substituent groups as well in the cages as within the cavities. The distances between the two side chains of consecutive molecules AA' or BB' (L-Phe C $\beta$  to one methyl C-atom) of  $4.12$  and  $3.92\text{\AA}$ , respectively, suggest a simultaneous close stacking of the successive substituent groups through the cavities.

The cohesion of the AA' and BB' associations is reinforced by short contacts involving the carboxyl groups of the amino-acids which are differently involved in intermolecular interactions (Table 3). In the association BB', O1B is at hydrogen bond distance from a secondary hydroxyl group of molecule B' (O1B-O32'). This is the sole intermolecular interaction between molecules B and B'. In the association AA', this interaction is mediated by a water molecule (WA5), itself involved in an intramolecular bridge between O1A and O64A. The intermolecular interaction O64A-O31A' and the hydrogen bond contact with WA5 cause the conformational change (C64, O64) which is *gauche-trans* in molecule A and *gauche-gauche* in molecule B, without disturbing the overall conformation of the substituents.

An interesting feature concerns the unique primary hydroxyl (O61) in *gauche-trans* conformation in both mol-

ecules, which is at intramolecular hydrogen bond distance from the amino acid nitrogen atom. This interaction (O61-N1) contributes to the geometry of the L-Phe backbone relative to the parent macrocycle.

At this point it is worthwhile commenting on how the Boc moiety affects the auto-inclusion which has been previously proposed in the phenylalanyl-amino- $\beta$ -CD derivatives<sup>10,12</sup>. The formation of an intermolecular host-guest complex is achieved as it was previously reported when the *tert*-butylthio is grafted on  $\beta$ -CD<sup>6</sup>, though in the present derivative the *tert*-butyl is attached with a longer length spacer arm. This intermolecular inclusion is accomplished with a non extended conformation of the Boc-L-Phe-NH group and excludes the possibility of an auto-inclusion of the aromatic moiety.

The O61-N1 interaction should be a structural characteristic independent of the crystal stacking and also solvent effect which might be retained in solution. As it should not be depend on the Boc effect, it might be a conformational feature of the L-Phe-amino- $\beta$ -CDs. It is remarkable that the observed L-Phe backbone conformation is compatible, in the absence of Boc, with an auto-inclusion of the aromatic moiety. This requires a change of only the  $\chi_1$  angle. Of course a conformational adaptation should be also needed to provide a better orientation of the phenyl moiety with respect to the macrocyclic ring, leading to a change of the  $\chi_2$  angle. However, the L-Phe C $\alpha$  atom being at 4.8Å above the macrocycle O4 plane, the phenyl ring could not be deeply included within the cavity.

## CONCLUSION

The monosubstitution of  $\beta$ -CD by a protected amino acid system leads to a novel self-aggregation of mono-substituted  $\beta$ -CD derivatives, arising from an unusual intermolecular host/guest interaction with regard to those previously reported. It has been shown that the more hydrophobic group (*tert*-butyl) is preferentially included. This behaviour may be considered as a model for selective processes between hydrophobic groups involving substituted cyclodextrins. Furthermore, a new type of structure is observed which maintains the L-Phe amino acid out of the cyclodextrin cavity but prevents it from being exposed to the aqueous environment exterior to the cyclodextrin chain structures.

The intermolecular inclusion process favors a non-extended conformation for the Boc-L-Phe-NH group, with

no large scale distortions of the macrocyclic ring. This might be applied either to provide suitable unusual conformation of small hydrophobic substrates or to prevent hydrophobic peptido monosubstituted  $\beta$ -CD derivatives from the auto-inclusion of apolar side-chain. However, the insertion of a longer length spacer arm between the macrocycle and the functional group is required to impose the peptido side-chain at the exterior of the cyclodextrin chain structure, as is needed in the design of systems having optimal function and selectivity in molecular biorecognition process.

## REFERENCES

- 1 Wenz, G.; *Angew. Chem. INT. Ed. Engl.* **1994**, *33*, 803–822.
- 2 Parrot-Lopez, H.; Leray, E.; Coleman, A.W.; *Supramol. Chem.* **1993**, *3*, 37–42.
- 3 Charpin, P.; Nicolis, I.; Rango de, C.; Coleman, A.W.; *Acta Cryst.* **1990**, *A46*, C169. Crystal Data: 6-amino-6-deoxy- $\beta$ -CD, a = 15.049, b = 10.365, c = 20.886Å,  $\beta$  = 109.73°, P2<sub>1</sub>, Z = 2; 6-azido-6-deoxy- $\beta$ -CD, a = 15.044, b = 10.274, c = 20.846Å,  $\beta$  = 109.89°, P2<sub>1</sub>, Z = 2.
- 4 Harata, K.; *Inclusion Compounds, Vol. 5*, Atwood, J.; Davies, J.E.D.; MacNicol D.D. Ed.; Oxford Univ. Press, **1991**.
- 5 Harata, K.; Trinadha Rao, C.; Pitha, J.; Fukunaga, K.; Uekama, K.; *Carbohydr. Res.* **1991**, *222*, 37–45.
- 6 Hirotsu, K.; Higuchi, T.; *J. Org. Chem.* **1982**, *47*, 1143–1144; Fujita, K.; Matsunaga, A.; Imoto, T.; *J. Am. Chem. Soc.* **1985**, *107*, 1790–1791.
- 7 Mentzafos, D.; Terzis, A.; Coleman, A.W.; Rango de, C.; *Carbohydr. Res.*, submitted.
- 8 Kamitori, S.; Hirotsu, K.; Higuchi T.; *J. Chem. Soc. Perkin Trans II* **1987**, 7–17.
- 9 Blasio di, B.; Pavone, V.; Natri, F.; Isernia, C.; Saviano, M.; Pedone, C.; Cucinotta, V.; Impellizzeri, G.; Rizzarelli, E.; Vecchio, G.; *Proc. Natl. acad. Sci. USA* **1992**, *89*, 7218–7221.
- 10 Parrot-Lopez, H.; Galons, H.; Coleman, A.W.; Djedaïni, F.; Keller, N.; Perly, B.; *Tetrahedron Asym.* **1990**, *1*, 367–370.
- 11 Takhashi, K.; Hattori K.; *Supramol. Chem.* **1993**, *2*, 305–308.
- 12 Nicolis, I.; Coleman, A.W.; *Supramol. Chem.*, submitted.
- 13 Navaza, J.; *Acta Cryst.* **1994**, *A50*, 157–163.
- 14 Sheldrick G.M.; *Program for crystal structure determination. SHELX76*. Univ. of Cambridge, England.
- 15 Jones T.A.; *J. Appl. Cryst.* **1978**, *11*, 268–272.
- 16 *SYBYL 5.10*, Tripos Inc., Missouri, U.S.A.
- 17 Saenger, W.; *Hydrogen Bonding in Biological Structures, Chap. 15*, 309–350, Jeffrey, G.A.; Saenger, W., Eds.; Berlin Springer-Verlag, **1991**.
- 18 Capasso, S.; Mazzarella, L.; Sica, F.; Zagari, A.; Cascarano, G.; Giacobozzo, C.; *Acta Cryst.* **1992**, *B48*, 285–290.
- 19 Doi, M.; In, Y.; Ikuma, K.; Inoue, M.; Ishida, T.; *Acta Cryst.* **1993**, *C49*, 1528–1530; Doi, M.; In, Y.; Tanaka, M.; Inoue, M.; Ishida, T.; *Acta Cryst.* **1993**, *C49*, 1530–1532.
- 20 Ashida, T.; Tsunogae, Y.; Tanaka, I.; Yamane T.; *Acta Cryst.* **1987**, *B43*, 212–218.
- 21 Walker, N.; Stuart, D.; *Acta Cryst.* **1983**, *A39*, 158–166.

## SUPPLEMENTARY MATERIALS:

## MOLECULAR RECOGNITION IN CYCLODEXTRINS.

THE X-RAY STRUCTURE OF 6<sup>A</sup>-BOC-L-PHENYLALANYLAMINO-6<sup>A</sup>-DEOXY- $\beta$ -CYCLODEXTRINFractional coordinates ( $\times 10^3$ ) and isotropic or equivalent thermal parameters ( $\times 10^2$ ) of the O-Waters with occupancy factors

	<i>x</i>	<i>y</i>	<i>z</i>	<i>U(iso/eq)</i>	
W(A1)	466 (1)	273 (1)	625 (1)	8 (1)	
W(A2)	86 (2)	739 (1)	673 (1)	8 (1)	Occupation=0.80
W(A3)	471 (2)	712 (1)	448 (1)	8 (1)	Occupation=0.75
W(A4)	238 (3)	681 (2)	778 (1)	10 (1)	Occupation=0.50
W(A5)	163 (2)	796 (1)	444 (1)	9 (1)	Occupation=0.66
W(A6)	481 (3)	730 (2)	593 (1)	9 (1)	Occupation=0.50
W(A7)	323 (3)	687 (2)	298 (1)	9 (1)	Occupation=0.50
W(A8)	208 (2)	182 (2)	358 (1)	10 (1)	Occupation=0.66
W(A9)	87 (3)	207 (2)	289 (1)	10 (1)	Occupation=0.50
W(A10)	372 (3)	208 (2)	690 (1)	9 (1)	Occupation=0.50
W(A11)	225 (5)	279 (4)	695 (3)	10 (3)	Occupation=0.25
W(A12)	434 (3)	444 (2)	703 (1)	9 (1)	Occupation=0.50
W(A13)	414 (4)	618 (3)	348 (2)	10 (2)	Occupation=0.33
W(A14)	392 (4)	686 (3)	688 (2)	8 (2)	Occupation=0.33
W(A15)	305 (3)	321 (2)	380 (1)	9 (1)	Occupation=0.50
W(A16)	384 (6)	372 (5)	358 (3)	11 (3)	Occupation=0.25
W(B1)	428 (3)	246 (2)	924 (1)	9 (1)	Occupation=0.50
W(B2)	160 (3)	299 (2)	783 (1)	10 (1)	Occupation=0.50
W(B3)	220 (2)	811 (2)	215 (1)	8 (1)	Occupation=0.50
W(B4)	435 (3)	754 (2)	907 (1)	8 (1)	Occupation=0.50
W(B5)	391 (3)	868 (2)	833 (1)	10 (1)	Occupation=0.50
W(B6)	412 (4)	294 (4)	43 (2)	7 (2)	Occupation=0.25
W(B7)	344 (3)	491 (2)	776 (1)	11 (1)	Occupation=0.50
W(B8)	431 (4)	98 (3)	141 (2)	10 (2)	Occupation=0.33
W(B9)	194 (5)	339 (4)	157 (2)	7 (2)	Occupation=0.25
W(B10)	78 (3)	769 (2)	829 (1)	8 (1)	Occupation=0.50
W(B11)	22 (3)	782 (3)	838 (1)	11 (2)	Occupation=0.50
W(B12)	279 (4)	289 (3)	106 (2)	11 (2)	Occupation=0.33
W(B13)	326 (5)	215 (4)	123 (2)	8 (2)	Occupation=0.25
W(C1)	135 (2)	730 (1)	281 (1)	9 (1)	Occupation=0.80
W(C2)	202 (2)	820 (2)	741 (1)	10 (1)	Occupation=0.66
W(C3)	326 (5)	91 (4)	212 (2)	9 (3)	Occupation=0.25
W(D1)	393 (5)	891 (4)	247 (3)	11 (3)	Occupation=0.25
W(D2)	466 (4)	925 (4)	160 (2)	11 (2)	Occupation=0.33